Tellus (1986), *38A*, 453–461

A cloud climatology for the South Atlantic derived from METEOSAT I images

By S. COULMANN, S. BAKAN* and H. HINZPETER, *Meteorologisches Institut der Universität Hamburg, Bundesstrasse 55, 2000 Hamburg 13, F.R. Germany*

(Manuscript received July 15; in final form January 13, 1986)

ABSTRACT

Statistics of total and high-level cloud amount (monthly average and standard deviations) over 5° × 5° areas have been derived for the South Atlantic between 0°–40°S and 10°E–35°W from METEOSAT I data. Glossy prints of all available noon images between February 1978 and November 1979 have been evaluated with a threshold method using the VIS and IR data. The main features of the cloudiness over the South Atlantic are the highly persistent boundary layer cloudiness in the eastern regions, the high cloud coverage in connection with the subtropical jet stream and the relatively low cloud coverage in the western regions. The cloudiness in the eastern regions undergoes a clear seasonal cycle with maximum cloud amounts during September–November and minimum in June, while in the other regions, the seasonal cycle is less evident. A remarkable amount of high level cloud has been found during all months in connection with the subtropical jet stream, and between December and May near the coasts.

1. Introduction

Clouds play a major rôle for the radiation balance of the planet, which itself is the most important process that drives the climate system. Incoming solar as well as emitted terrestrial radiation is strongly influenced by emission, absorption and scattering of radiation by clouds. As a basis for climate studies and modelling, a knowledge of temporal and spatial distribution of clouds is most important. Progress towards understanding the earth's climate is currently hindered by the limited knowledge of the global cloud distribution and its variability (Rossow, 1981). There is at present no unique and generally agreed global cloud climatology (Hughes, 1984).

Only the advent of a dense net of satellites provides the possibility of systematic cloud coverage monitoring. To facilitate the use of routine satellite data, the International Satellite Cloud Climatology Project (ISCCP) was launched. But while this project started with data collection in July 1983, considerably more data are available dating back into the 1970's. The European geostationary satellite METEOSAT, for example, has provided full disk images of the earth since February 1978.

This older data from METEOSAT I is used in the present effort to derive a cloud climatology of the South Atlantic. The choice of this area is for several reasons. Regional cloud statistics have been compiled by many authors using a variety of data sources, but the majority of these are for the northern hemisphere. Not much effort has been put into evaluating the METEOSAT I data for the southern hemisphere, especially not into the evaluation of longer time series. On the other hand, recent research shows the climatological importance of the subtropical areas with widespread boundary layer cloudiness. The marine stratus and stratocumulus systems especially have a strong influence on climate. Randall et al. (1984) estimate, that a mere 4% increase in the area of the globe covered by low level stratus clouds would be sufficient to offset the 2–3 K

* *Max-Planck-Institut für Meteorologie, Hamburg, F.R. Germany*

predicted rise in global temperature due to a doubling of CO_2. Also there is a well-known deficiency in GCM's to forecast this type of clouds correctly. This, together with an almost ideal observation angle from METEOSAT, is the motivation to make a statistical study of the cloud coverage over the South Atlantic.

2. Data sources

In contrast to most of the satellite image data analyses, this evaluation is not based on the original digital image data on tape, but black and white prints of the images, produced from the European Space Operations Centre (ESOC) in Darmstadt. This was mostly done for financial and logistic reasons, in order to be able to acquire and evaluate enough data for statistically meaningful results. The South Atlantic region of the images was then digitized on a standard Quantimet 720/23 image proccessing facility (Cambridge Instruments). One pair of visible (VIS: 0.4–1.1 μm) and infrared (IR: 10.5–12.5 μm) images have been processed for noon of each day between February 1978 and November 1979. For some days, the pictures were not available due to, e.g., data-transmission failure or had to be dismissed due to poor photographic quality. Therefore, only 82% of the 668 days could be analyzed. Only in February, March, May, October 1978 and June 1979 were more than 30% (but less than 50%) of the data missing. The images from 12.00 GMT (Slot 24), which corresponds to 10.00–12.00 LT, were chosen for two reasons. Firstly, just at this time, the whole South Atlantic region is illuminated by the sun and secondly, only slot 24 is routinely processed as a negative image by ESOC. There are some remarkable differences between the original image data and the digitized data received from the prints. The glossy prints provided by ESOC contain 32 grey levels. This is less than the original grey scale resolution of the satellite digital data and less than the 64 grey levels of the image processing system. The data differ in spatial resolution too. Each original METEOSAT image is composed of 2500 lines and 2500 picture elements with a spatial resolution of 5 km at the subsatellite (SSP) point. The resolution of the digitized prints comes to 10 km at the SSP. This is nearly the same resolution as used in the B1-data set which is produced for the ISCCP.

The present evaluation is restricted to the area from the equator to 40°S and from 10°E to 35°W. This region was chosen to guarantee sun zenith angles and satellite viewing angles less than 70° for the whole area. The region is split into 5° × 5° subregions, for which the 2-dimensional histogram is built from the VIS and IR data and stored for further reference. Each of these histograms is made up of roughly 2000 data points.

One special problem arises in this procedure, as not all the images are developed photographically in the same way. This prevents identical grey levels in different images to be compared directly. They have to be transformed to the original 32 grey levels available in the print by use of the calibration grey scale displayed on each image.

One general problem in determining cloud cover from satellite data results from partially filled fields of view. Clouds may be either smaller than the instrument's field of view (5 km) or they may be aligned so that some picture points (pixels) are only partially covered by cloud edges. The same problem occurs in the digitizing procedure. A picture point from the Quantimet video scanner covers several pixels of the print. So some picture points are neither completely cloud covered nor completely clear. This problem has to be considered when choosing the analysis method.

3. Analysis method

Several analysis methods have been used in the literature to derive cloud coverage from satellite images. The most refined method seems to be the cluster method, where the clustering of data points in a 2-dimensional histogram is directly analysed. This allows for a rather clear separation of cloudy and noncloudy areas and of several cloud types. Simmer (1981) shows some successful examples for this method. But he also demonstrates that additional information from other data sources (e.g., climatological data) and from radiative calculations is necessary for a correct interpretation of the clusters. Also the complete grey scale resolution of the original satellite data is important for a sensible cluster separation. For the present investigation, this sophisticated method seems not feasible due to the rather coarse data material.

Spatial coherence methods use the spatial structure of the IR-radiance field to identify radiances associated with cloud-free or completely cloud-covered fields of view (Saunders, 1985; Coakley and Bretherton, 1982). These coherence methods are applicable for regions which contain both completely clear and completely cloudy portions that span several fields of view. To meet this condition, especially in the case of broken clouds, a spatial resolution of less than 5 km at the SSP is necessary. Due to the rather coarse spatial resolution of the digitized prints and the reduced grey scale, the application of a coherence method seems inappropriate for the present investigation. Therefore, a threshold method is used, which in its simplicity allows for the analysis of a large number of images, which is necessary to receive reliable statistical results. The threshold method is based on the possibility of finding a grey value in the image, such that all pixels with grey tones below this value are classified as ocean and all pixels with higher grey tones as clouds. The main problem with this procedure comes from the partially filled fields of view. Generally there are several grey tones between the values of completely cloud-free ocean pixels and completely cloud-covered pixels. A careful treatment of these mixed pixels is necessary, to avoid a systematic over- or underestimation of the cloud cover.

In a first step, the visible image is used to determine the total cloud cover. This is done by setting an empirically determined, fixed-threshold grey value for the separation of cloudy and noncloudy areas (Fig. 1). This procedure works fine as the underlying surface is ocean in the whole analysis region and as the albedo difference is always large in the visible image between clouds and ocean. The albedo of clouds and ocean measured by satellites depends on the solar zenith angle and the satellite viewing angle. This dependence is considered in detail by Gube (1982) for METEOSAT data. For the South Atlantic region between 0°–40°S and 10°E–35°W at 1200 GMT, the albedo of the ocean outside sunglint areas is always below 10%, the average

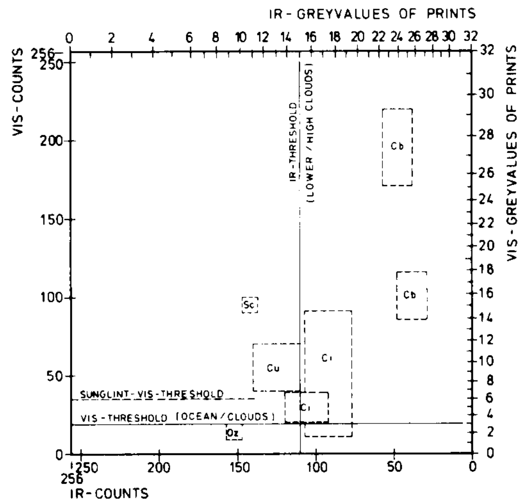

Fig. 1. Histograms from several sources (see text) and VIS and IR thresholds for the present study. The original IR/VIS-counts from the radiometer and the corresponding 32 grey values of the prints are given on the axes.

value is 5%. The seasonal variation of ocean albedo is neglected, as it accounts for less than one grey value. The albedo of clouds generally exceeds 20%; only thin cirrus may have a smaller albedo. Under these conditions, it is possible to use a fixed grey level threshold to separate cloudy from noncloudy pixels in the visible image. By setting this threshold, the problem of the mixed pixels is considered. The comparison of VIS histograms for completely cloud-free, partially-cloud-covered, and overcast areas shows that the corresponding grey values of mixed pixels in the VIS image are 3 and 4. The threshold is set to the value 3, so the relatively dark pixels are classified as ocean and the brighter ones as cloud with the hope that possible errors offset each other.

The sunlight near the subsatellite point, however, needs special treatment. In the visible image, sunglint areas show grey values that are typical for clouds. The sunglint region can be separated from cloudy areas by comparison with the grey values in the corresponding infrared image. The sunglint correction is done by setting up the VIS threshold to the grey value 6 (Fig. 1) for sunglint areas. In addition to all pixels, which show grey values from 1 to 3 in the VIS image, pixels with higher grey tones up to 6 are classified as ocean, if their corresponding IR values coincide with the ocean grey value of the area.

The IR-ocean grey value of the considered 5° × 5° area is determined by the minimum grey value of this and the 8 neighbouring areas. The ocean grey value varies with the angle of observation due to enhanced emission of atmospheric constituents in a slant path and the variable sea surface temperature.

In contrast to the VIS-image, it is not possible to find definite threshold grey values in the IR-image which allow a fairly reliable determination of areas covered with low, medium or no clouds. Due to their small temperature difference, ocean and low clouds correspond to neighbouring values in the IR-grey scale. While medium level clouds can sometimes clearly be distinguished, they often show grey values only slightly larger than low-level clouds. This fact prohibits the reliable determination of medium-level cloud area in the present routine analysis.

On the other hand, the grey values of high-level cloud types such as cirrus and cumulonimbus are well separated from low cloud types in the grey scale of the IR-photos. Experience shows that the separation of high-level clouds from other clouds and ocean is possible with a threshold 5 grey tones higher than the ocean value.

In the case of semi-transparent high-level clouds their grey values may be less than the IR-threshold leading to an underestimation of the high-level cloud amount. While it is hardly possible to quantify this error, the comparisons discussed in Subsection 4.2 show satisfactory agreement of the present values with other data sources. In addition to the chosen thresholds, Fig. 1 shows some typical 2-dimensional histograms for several regions in the South Atlantic as found by Billing et al. (1980), Desbois et al. (1982) and Duvel and Kandel (1985) from different METEOSAT images. The chosen thresholds prove to be suitable for separating clouds from ocean and high clouds from other cloud types.

4. Results

4.1. Monthly mean cloudiness and variability

From the daily values of total and high level cloud amount at 12.00 GMT, monthly averages and standard deviations have been computed for each 5° × 5° region. In Fig. 2, for example, isolines of these values for January, April, July and October 1979 are shown. The main features of the monthly mean cloudiness over the South Atlantic are the low cloud coverage in the western region ($N < 50\%$) and the high coverage ($N > 60\%$) in the eastern and southern regions. The cloud coverage of the latter 2 areas differs significantly in cloud type. In the southern part, which is influenced by the subtropical jet stream, high-level clouds make a remarkable contribution to total coverage in all months. In the eastern parts, boundary layer cloudiness such as stratocumulus layers or closed convection cells predominate. The cloud amounts in this region undergo a clear annual cycle, with maxima in September–November and minima between May and July. The cloud coverage between 5°E–5°W and 10°S–20°S is highly persistent during the period August–November, indicated by the rather small standard deviations of the monthly mean cloud amounts ($\sigma < 15\%$). Otherwise the standard deviations are always high.

The high-level cloud distribution shows a clear annual variation, too. In July and October, high-level clouds occur only south of 20° latitude and the amounts are smaller than in January and April. They appear only in connection with the subtropical jet stream or near the coasts, as cumulonimbus with cirrus canopies. In the eastern and central regions, high clouds occur rarely. This rapid change in cloud type causes the conspicuous high gradients in the standard deviations of the high-level clouds.

4.2. Reliability of the results

Unfortunately, little data exist, to check the results of the present investigation. Generally, it is very difficult to compare the available cloud statistics due to differences in the basic data sets. Some statistics are compiled from surface observations, others from satellite data or from both sources; various temporal and spatial resolutions are used. The data from Hoeflich (1984), who derived average monthly cloud amounts from a large sample of ship observations, seem to be comparable with the present evaluation. Since 1961, all ship observations of the South Atlantic are collected and evaluated by the Seewetteramt in Hamburg, FRG. Additionally observations from a period of about 100 years have been taken

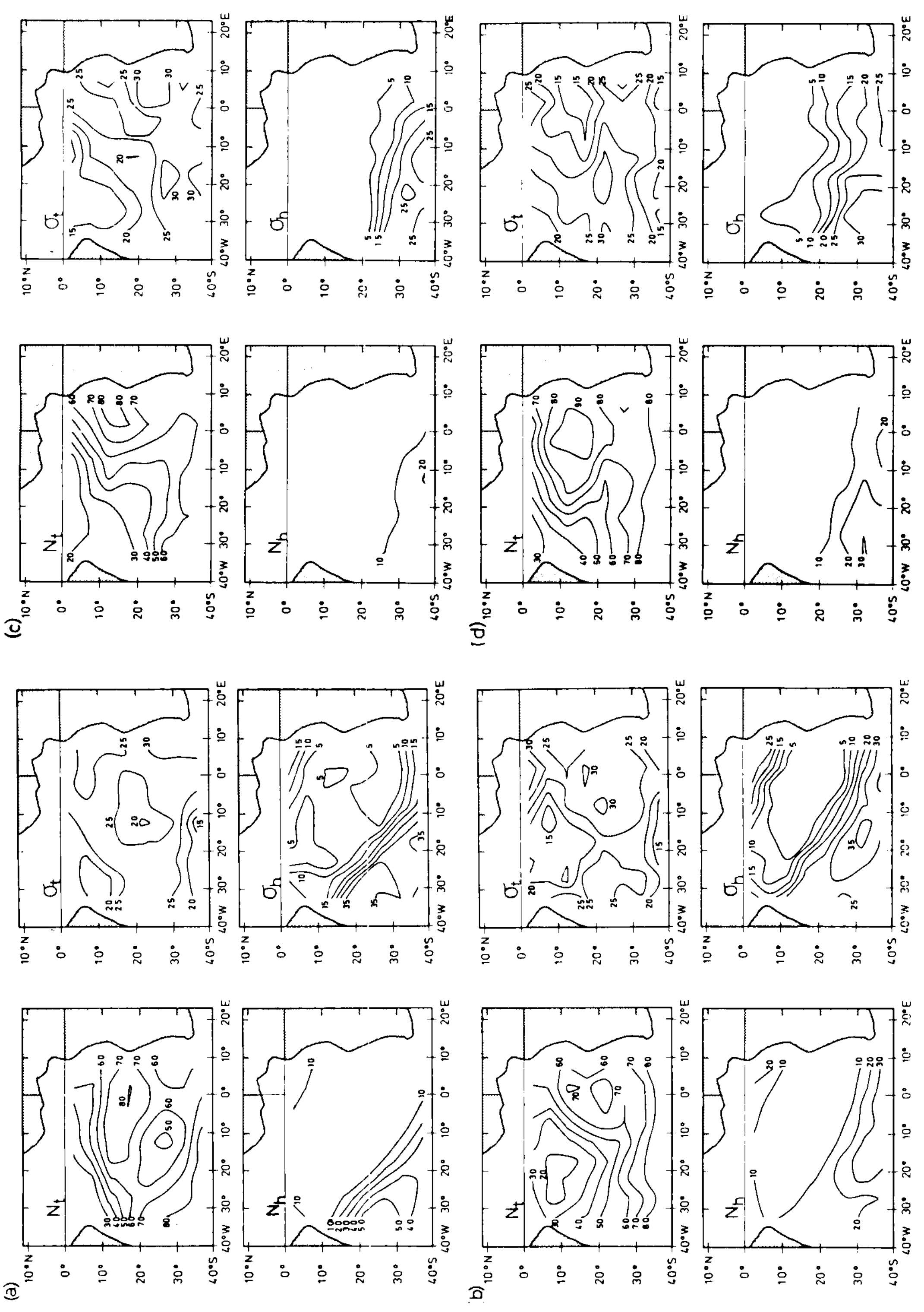

Fig. 2. Monthly mean and standard deviation of total (N_t, σ_t) and high-level (N_h, σ_h) cloud amount at 12.00 GMT for (a) January, (b) April, (c), July and (d) October 1979.

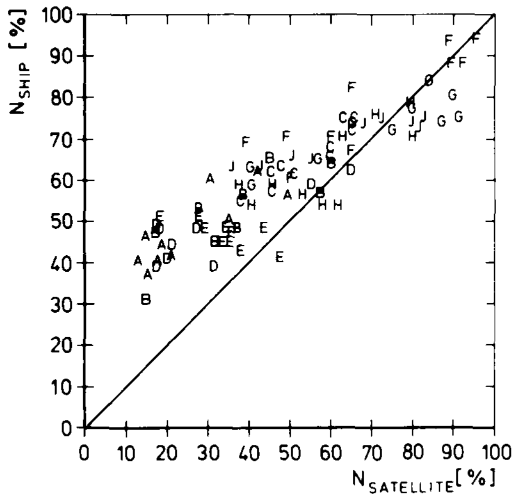

Fig. 3. Monthly mean cloud amounts from ship observations (Hoeflich, 1984) versus METEOSAT I results of the present study (1978/1979 averages). Letters A through J indicate different analysis areas (see Hoeflich).

into consideration by Hoeflich. Some of his analysis areas coincide with regions of the present investigation. In Fig. 3, the monthly averaged cloud amounts from Hoeflich are displayed against the corresponding values from the METEOSAT data. In several studies, systematic differences between cloud amounts derived from satellite and from ground observations have been encountered. Malberg (1973) carried out a comparison of the cloud coverage derived from ESSA 8 pictures with data from surface observations at 29 synoptic stations between 30° N–70° N, 40° W–70° W for the period December 1, 1967–November 30, 1970. He found that the cloud amounts derived from surface observations are always greater than the values derived from satellite data. For the observed cloud amounts (between 50%–80%) he found an average difference of about 15% between 30°–40° N. Similar agreement is found between the data of Hoeflich and the present results. In addition, the observed differences in Fig. 3 are partially due to different observation periods. Saunders (1985) derived the total cloud amount for a 7-month period of METEOSAT data from 1983 over the region between 40° N–40° S, and 40° W–40° E. As examples, he presents the monthly mean values of 250 × 250 km² areas for April, July and October, 1983. These results are in good qualitative agreement with the main features of the cloudiness over the South Atlantic in 1978 and 1979 found in the present investigation.

Global cloud amounts for high-level clouds are shown by Barton (1983), analysed from NIMBUS 5 data for the time period December 1972 to June 1975. In agreement with these results, the present investigation shows cloud amounts above 20% only in the region of the subtropical jet during all months and along the Brazil and African coast near the equator from December to May.

A cloud climatology derived from noon images may not necessarily be representative for the whole day. As the present analysis technique relies on both the VIS and IR image, it does not permit a study of the change in cloudiness throughout the whole day. But, a preliminary analysis of 3-hourly images on 5 days in April 1982 with an interactive IR-threshold method does not show any systematic deviations for 24 areas (5° × 5°) between 10°–30°S and 10°E–20° W. The average deviation is less than 1%, with maximum over- and underestimation of less than 15%. Another example of the daily cycle of low-level cloudiness in the South Atlantic derived from the METEOSAT B1-data set is given by Saunders (1985) for an area of 250 × 250 km² located at 16°S, 3° W. For April 1983, he shows that the noon value overestimates the daily mean low cloudiness by 10%. Duvel and Kandel (1985) give a few results on the daily variability of cloud coverage for the tropical South Atlantic between 10°E and 20° W derived from the original METEOSAT data of the periods January 27–29 and August 2–4, 1979. For their 2 analysis areas in the South Atlantic, the low-level cloud amount (which is nearly the total cloud amount) at 12 GMT slightly underestimates the daily mean low-level cloud coverage by less than 6% in both months. Minnis and Harrison (1984) analysed GOES data of November 1978 for the South Pacific. They present the daily variation of cloud amount in 32 areas of 250 × 250 km² between 9°–18°S and 80°–99° W. Diurnal variations in total cloudiness are most substantial over regions where clouds predominantly occur at one level in the atmosphere, such as the cloudiness over much of the southeastern Pacific. From the results of Minnis and Harrison, the difference between the daily mean total cloud coverage and the cloud amount at 12.00 LT has been derived. The noon value always underestimates the daily mean cloud coverage with an average difference of 9%. As a consequence of these different studies, the cloud amount derived from 12.00 GMT images and the daily mean cloud coverage should agree within 10% on average.

4.3. *Time series of cloud coverage*

The monthly mean cloud amounts and standard deviations give information about the geographical cloud distribution and its variability. But these average values do not represent the most probable cloud amounts of a region, because cloud coverage does not follow the normal distribution. The frequency distributions have been calculated from the daily cloud amounts of the complete analysis period for each 5° × 5° region. They show quite different shapes with 3 typical forms. Examples of these are shown in Fig. 4.

In the eastern and southern regions of the South Atlantic, the frequency distribution is J-shaped with high cloud amounts dominating. In the north-western part, low amounts are more frequent, and the frequency distribution is reverse J-shaped. In the central areas, all cloud amounts occur with roughly the same probability.

A continuous distribution able to reproduce the different shapes is the beta-distribution (Falls, 1974), the form of which is given by

$$f(x) = \frac{\Gamma(a+b)}{\Gamma(a)\cdot\Gamma(b)} x^{a-1} (1-x)^{b-1},$$

where $0 \leq x \leq 1$; a, $b > 0$, and Γ represents the gamma-function. The parameters a and b determine the shape of the distribution. For each 5° × 5° area, these parameters are estimated by varying a and b until the rms-difference between the β-distribution and the observations is minimized. Examples for the quality of the fit are shown in Fig. 4. The differences between the observed frequencies and the β-function approximation are generally small; the average value is 2.5%. The maximum difference of 11% is found in the south-west corner of the analysis region. In Fig. 5, the parameters a, b are shown for the whole area.

While the frequency distributions yield information about the probable cloud amount, the temporal persistence of the cloud coverage is given by the autocorrelation function (ACF). It

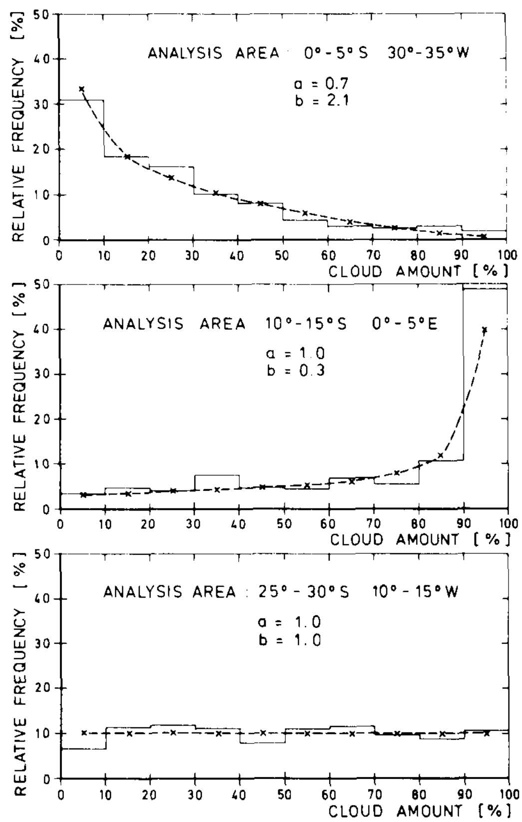

Fig. 4. Typical frequency distributions of cloud coverage (bar diagram) and their β-function approximations (dashed lines).

was calculated from the daily cloud amounts for each 5° × 5° area. The ACF in the region of the boundary layer cloudiness differs considerably from that in the other parts. Here the function decreases slowly, falling below 1/e after about 20 days. The decrease in the western and southern regions is much faster, the value 1/e is already reached after 1–2 days. This indicates highly persistent cloudiness in the eastern area and rapid changes from day-to-day in the other parts.

As a measure of the persistence, a decorrelation-time is computed as the integral over the ACF between zero and that time-lag where the ACF falls below zero. This integral is identical to the integral over a constant ACF of value 1 between zero and the decorrelation-time. Fig. 6 shows the decorrelation-time for each 5° × 5° region. The largest values of 24 days are found in

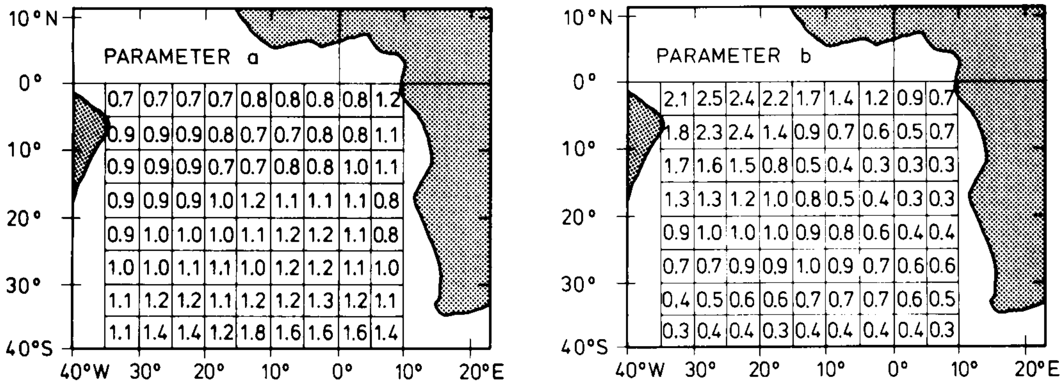

Fig. 5. Parameters *a*, *b* of the β-distribution which approximates the observed frequency distribution (Feb. 1978–Nov. 1979) of the total cloud amount.

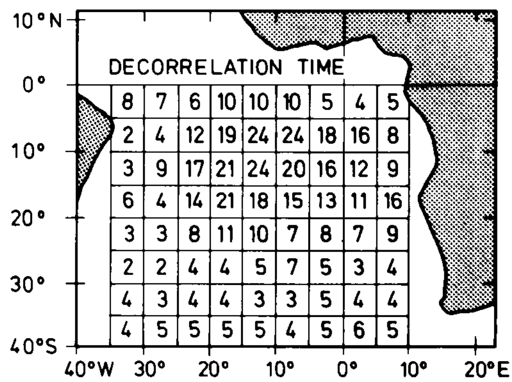

Fig. 6. Spatial distribution of the decorrelation-time (in days) of total cloudiness.

the regions of the boundary layer cloudiness, stressing again their high persistence.

5. Concluding remarks

Cloud statistics for the South Atlantic were derived from 2 years of METEOSAT data. While the use of photographic prints, originally chosen for financial and logistic reasons, did not reliably allow a separation of low- and medium-level clouds, the results for the total and high-level cloud coverage appear to have accuracies comparable to those obtained by analysing the original satellite data. The results underline the importance of the boundary layer cloudiness for the climate. During the whole year, layered or broken cloud fields are observed in the eastern South Atlantic with high cloud amounts of about 70% and high persistence.

The parameterization of boundary layer cloudiness especially in the eastern regions of the oceans is still an unsolved problem in climate modelling. Longer time series of cloud coverage are necessary for the development and validation of cloud parameterization schemes. While METEOSAT I data cover a period of nearly 2 years, an expansion over more years is desirable to improve statistical reliability. The investigation will be extended to METEOSAT II images. In addition, this would then allow a comparison with the results from the more recently started ISCCP.

The present statistics are made from noon images, which are assumed to represent the daily mean cloud coverage as suggested by comparison with other studies. Unfortunately, only few investigations of the daily cycle of cloudiness have been published. The removal of this observational deficiency, especially in the eastern ocean regions with the long-lasting boundary layer cloudiness, is urgent for sampling accuracy considerations. Recently, indications of a nonlinear relation between radiative quantities such as planetary albedo and cloudiness in broken cloud fields have been published (Schmetz, 1984). As this nonlinearity is especially large for stratocumulus fields with high cloud amounts, it is important to put more effort into evaluating the daily cycle of boundary layer cloudiness.

6. Acknowledgement

The investigation was sponsored by the BMFT as part of the national climate research program of the FRG. Special thanks go to Dipl.-Met. D. Schriever for extensive support in the image processing, to S. Schmidt, M. Knobelsdorf, M. Wefers for assisting in the routine analysis, and to B. Zinecker for kindly typing the manuscript.

REFERENCES

Barton, I. J. 1983. Upper level cloud climatology from an orbiting satellite. *J. Atmos. Sci. 40*, 435–447.

Billing, H., Haupt, I., Koslowsky, D. and Tonn, W. 1980. On the development of cloud structures on different scales. *Ann Meteorol (Neue Folge), nr. 15*, DMG-Tagung Berlin 1980, (in German).

Coakley, J. A. and Bretherton, F. P. 1982. Cloud cover from high resolution scanner data: detecting and allowing for partially filled fields of view. *J. Geophys. Res. 87*, 4917–4932.

Desbois, M., Seze, G. and Szejwach, G. 1982. Automatic classification of clouds on METEOSAT imagery: Application to high level clouds. *J. Appl. Meteorol. 21*, 401–412.

Duvel, J. P. and Kandel, R. S. 1985. Regional scale diurnal variations of outgoing infrared radiation observed by METEOSAT. *J. Clim. Appl. Meteorol. 24*, 335–349.

Falls, L. W. 1974. The beta distribution: a statistical model for world cloud cover. *J. Geophys. Res. 79*, 1261–1264.

Gube, M. 1982. Radiation budget parameters at the top of the earth's atmosphere derived from METEOSAT-data. *J. Appl. Meteorol. 21*, 1907–1921.

Hoeflich, O. 1984. Climate of the South Atlantic Ocean. In: *Climates of the oceans. World survey of Climatology 15*, ed: H. Van Loon.

Hughes, N. A. 1984. Global cloud climatologies: a historical review. *J. Clim. Appl. Meteorol. 23*, 724–751.

Malberg, H. 1973. Comparison of mean cloud cover obtained by satellite photographs and ground based observations over Europe and the Atlantic. *Mon. Wea. Rev. 101*, 893–897.

Minnis, P. and Harrison, E. F. 1984. Diurnal variability of regional cloud and clear-sky radiative parameters derived from GOES data. Part II. *J. Clim. Appl. Meteorol. 23*, 1012–1031.

Randall, D. A., Coakley, J. A., Fairall, C. W., Kropfli, R. A. and Lenschow, D. A. 1984. Outlook for research on subtropical marine stratiform clouds. *Bull. Amer. Soc., 65*, 1290–1301.

Rossow, W. B. Ed. 1981. Clouds in climate; modelling and satellite observation studies. Report of workshop held at NASA Goddard Institute of Space Phys. New York, 222 pp.

Saunders, R. W. 1985. Monthly mean cloudiness from METEOSAT II. *J. Clim. Appl. Meteorol. 24*, 114–127.

Schmetz, J. 1984. On the parameterization of the radiative properties of broken clouds. *Tellus 36A*, 417–432.

Simmer, C. 1981. Investigation of spatial sampling of satellite data with the aid of two dimensional histograms. Diplomarbeit, University of Cologne (in German).